Proceedings of HT-FED2004:
2004 ASME Heat Transfer/Fluids Engineering Summer Conference
July 11-15, 2004, Charlotte, North Carolina, USA

HT-FED2004-56127

APPLICATIONS OF THE LAGRANGIAN DYNAMIC MODEL IN LES OF TURBULENT FLOW OVER SURFACES WITH HETEROGENEOUS ROUGHNESS DISTRIBUTIONS

Elie Bou-Zeid
Department of Geography and Environmental Engineering
and
Center for Environmental and Applied Fluid Mechanics,
Johns Hopkins University

Charles Meneveau
Department of Mechanical Engineering
and
Center for Environmental and Applied Fluid Mechanics,
Johns Hopkins University

Marc B. Parlange
Department of Geography and Environmental Engineering
and
Center for Environmental and Applied Fluid Mechanics,
Johns Hopkins University

ABSTRACT

We study turbulent flow over surfaces with varying roughness scales, using large eddy simulation (LES). The goal is to use LES results to formulate effective boundary conditions in terms of effective roughness height and blending height, to be used for RANS. The LES are implemented with the dynamic Smagorinsky model based on the Germano identity. However, as is well-known, when this identity is applied locally, it yields a coefficient with unphysically strong fluctuations and averaging is needed for better realism and numerical stability. The traditional approach consists of averaging over homogeneous directions, for example horizontal planes in channel flow. This requirement for homogeneous directions in the flow field and the concomitant inability to handle complex geometries renders the use of this model questionable in studying the effect of surface heterogeneity. Instead, a new version of the Lagrangian dynamic subgrid-scale (SGS) model [1] is implemented. A systematic set of simulations of flow over patches of differing roughness is performed, covering a wide range of patch length scales and surface roughness values. The simulated mean velocity profiles are analyzed to identify the height of the blending layer and used to measure the effective roughness length. Extending ideas introduced by Miyake [2] and Claussen [3], we have proposed a simple expression for effective surface roughness and blending height knowing local surface patch roughness values and their lengths [4]. Results of the model agreed well with the LES results when the heterogeneous surface consisted of patches of equal sizes. The model is tested here for surfaces with patches of different sizes.

INTRODUCTION

Flows over surfaces with abrupt changes in surface roughness and heterogeneous roughness distributions occur in a wide range of engineering applications involving turbulent flows and in the environment (Atmospheric Boundary Layer flow). Consequently, the effect of variability in surface roughness on boundary layers continues to be the subject of numerous studies [5-9].

These studies attempt to understand and quantify the flow disturbances caused by the roughness change. In addition, a parameterization of the effect of heterogeneity is often desirable; for example, numerical simulations that cannot resolve the heterogeneity scale need to model its effect on resolved scales. Analytical and experimental techniques have been traditionally used to tackle the heterogeneity problem. More recently, numerical techniques, particularly Large-Eddy Simulation, has become increasingly popular as a tool for a physical understanding of the dynamics of the blending phenomena over heterogeneous surfaces [9-15]. This paper continues this previous body of work by using LES, with a new generation model for subgrid-scale stresses, to test a new parameterization for heterogeneous surfaces at high Reynolds numbers.

LARGE EDDY SIMULATION AND THE LAGRANGIAN DYNAMIC SGS MODEL

Large Eddy Simulation assumes that the largest eddies contain most of the energy and are responsible for most of the transport of momentum and scalars. LES consists of solving the Navier-Stokes equations with eddies smaller than the filter size excluded, whereas eddies larger than the filter size can be resolved [16]. The spatial filtering of the Navier-Stokes

equations gives rise to a subgrid-scale (SGS) flux term σ_{ij}; it represents the effect of small eddies that are filtered out on the resolved scales of motion. The modeling of this term is required to close the LES system of equations, which can be written in rotational form as

$$\frac{\partial \tilde{u}_i}{\partial t} + \tilde{u}_j \left(\frac{\partial \tilde{u}_i}{\partial x_j} - \frac{\partial \tilde{u}_j}{\partial x_i} \right) = -\frac{1}{\rho} \frac{\partial \tilde{p}^*}{\partial x_i} - \frac{\partial}{\partial x_j} \tau_{ij} + \widetilde{F}_i \quad , \quad \frac{\partial \tilde{u}_i}{\partial x_i} = 0 \,. \quad (1)$$

where a tilde (˜) denotes filtering at the grid scale Δ, u_i is one of the three components of the velocity vector, τ_{ij} is the deviatoric part of the SGS stress tensor σ_{ij}, the symmetric part being lumped into the pressure term

$$\tilde{p}^* = \tilde{p} + \frac{1}{3}\rho\sigma_{kk} + \frac{1}{2}\rho \tilde{u}_j \tilde{u}_j \,. \quad (2)$$

Since here we consider flows with very high Reynolds number well above the viscous sublayer (not wall-resolved LES [17]), the viscous term is not included in the LES equations used here. F_i is the external forcing; in this study for example, it is the mean streamwise pressure gradient forcing.

A widely used model for the SGS stress term is the viscosity-type Smagorinsky model which expresses the SGS flux as a function of the resolved strain rate tensor $\tilde{S}_{ij}$ using

$$\tau_{ij}^{smag} = -2(c_{s,\Delta}\,\Delta)^2 \left|\tilde{S}_{ij}\right| \tilde{S}_{ij} \quad \text{and} \quad \tilde{S}_{ij} = 0.5\left(\partial_j \widetilde{u_i} + \partial_i \widetilde{u_j}\right) \quad (3)$$

where Δ is the grid size. The only unknown in the above expression is the Smagorinsky coefficient $c_{s,\Delta}$. The traditional approach is to use a constant coefficient estimated from the theory of isotropic homogeneous turbulence to be about 0.17 [18]. However, turbulence near a wall cannot be assumed isotropic and homogeneous and hence the appropriate value for c_s may differ from 0.17.

The dynamic approach 'measures' the model coefficient dynamically during the simulation by using information from the smallest resolved scales [19]. The approach uses the assumption of scale-invariance, $c_{s,2\Delta} = c_{s,\Delta}$, by applying the coefficient measured from the resolved scales to the subgrid-scale range [20]. However, scale-invariance near the grid-filter scale Δ does not always hold. The coefficient depends strongly on scale when Δ tends to the integral scale (as occurs in the first few grid-points near the ground in LES of wall bounded flows that does not resolve the viscous sublayer). To account for scale effects, scale-dependent formulations have been successfully implemented for atmospheric boundary layer (ABL) flows by Porté-Agel *et al.* [21]. A power-law behavior is assumed for the scale dependence of c_s: $c_{s,\Delta} \sim \Delta^{\Phi}$ or $c_{s,2\Delta} \sim \beta\Delta^{\Phi} = 2^{\Phi}\Delta^{\Phi}$. The case $\Phi=0$ (i.e. $\beta=1$) corresponds to the scale-invariant standard dynamic model.

In Porté-Agel *et al.* [21], the scaling coefficient β itself was obtained dynamically using an additional filtering operation at a scale 4Δ. In this work, for computational simplicity a dynamic computation of β is avoided. Instead, the vertical profile of β as a function of z/Δ is taken from Porté-Agel *et al.* [21] and imposed as

$$\beta = 1 - 0.65\, e^{-0.7 z/\Delta} \,, \quad (4)$$

z being the distance from the surface. The dynamic model, even its scale-dependent version, yields a coefficient with strong fluctuations and averaging is required for numerical stability. The standard approach [19] averages over homogeneous directions, for example horizontal planes in wall-bounded flows. This requirement for homogeneous directions in the flow field and the concomitant inability to handle complex geometries renders the use of this model questionable in studying the effect of surface heterogeneity. Instead, a new version of the so-called Lagrangian dynamic SGS model [1] is used here.

In this approach, averages are obtained in time following fluid pathlines rather than over homogeneous directions. The Lagrangian model is very well suited for applications with heterogeneous spatial conditions since it preserves local variability, preserves Galilean invariance, and does not require homogeneous directions. The model starts from the Germano identity [19] that relates SGS stresses at different scales

$$L_{ij} = T_{ij} - \hat{\sigma}_{ij} = \widehat{\tilde{u}_i \tilde{u}_j} - \hat{\tilde{u}}_i \hat{\tilde{u}}_j \,, \quad (5)$$

where T_{ij} is the SGS stress at a scale 2Δ and L_{ij} is the resolved SGS stress tensor defined from scales intermediate between Δ and 2Δ. Filtering at a scale 2Δ is denoted by a hat (^). L_{ij} can be computed exactly from the resolved velocity field. Using the Smagorinsky model to express the deviatoric SGS stresses T^D_{ij} and τ_{ij} yields an error induced by the use of the Smagorinsky model.

$$e_{ij} = L^D_{ij} - (T^D_{ij} - \widehat{\tau_{ij}}) = L^D_{ij} - c^2_{s,\Delta} M_{ij} \,, \quad (6)$$

where $M_{ij} = 2\Delta^2 \left[\widehat{\left|\tilde{S}\right| \tilde{S}_{ij}} - 4\beta \left|\hat{\tilde{S}}\right| \hat{\tilde{S}}_{ij} \right]$.

In the Lagrangian SGS model, the coefficient $c_{s,\Delta}$ is obtained by minimizing the weighted time average of the squared error over pathlines. Using an exponential weighting function in time, as well as a simplified numerical treatment of the resulting relaxation transport equations (see [1] for details), we obtain

$$c^2_{s,\Delta} = \frac{\mathcal{I}_{LM}}{\mathcal{I}_{MM}} \,, \quad (7)$$

where

$$\mathcal{I}^{n+1}_{MM}(\boldsymbol{x}) = \varepsilon\, [M_{ij} M_{ij}]^{n+1}(\boldsymbol{x}) + (1-\varepsilon)\mathcal{I}^{n}_{MM}(\boldsymbol{x} - \tilde{\boldsymbol{u}}^n \Delta t)$$

$$\mathcal{I}^{n+1}_{LM}(\boldsymbol{x}) = \mathrm{H}\left\{ \varepsilon [L_{ij} M_{ij}]^{n+1}(\boldsymbol{x}) + (1-\varepsilon)\mathcal{I}^{n}_{LM}(\boldsymbol{x} - \tilde{\boldsymbol{u}}^n \Delta t) \right\};$$

$$\varepsilon = \frac{\Delta t / T^n}{1 + \Delta t / T^n} \,, \quad \Delta t = \text{time step},$$

$T^n = 1.5\Delta(\mathcal{I}^n_{LM}\mathcal{I}^n_{MM})^{-1/8}$ is the relaxation time scale used in the exponential weighting (allowing the model to allocate a higher weight to its recent history), and H(x) is the ramp

function needed to ensure that small numerical errors do not lead to negative $\mathcal{I}_{LM}$.

LES OVER HETEROGENEOUS SURFACES

Several simulations are performed to understand the effect of surface heterogeneity on the flow. The characteristics of the surface are varied and, for each simulation, the blending height (h_b) and effective surface roughness ($z_{o,e}$) are determined from LES results. Fig. 1 depicts the simulation domain and the main parameters used in the simulations; it illustrates an example with two unequal patches.

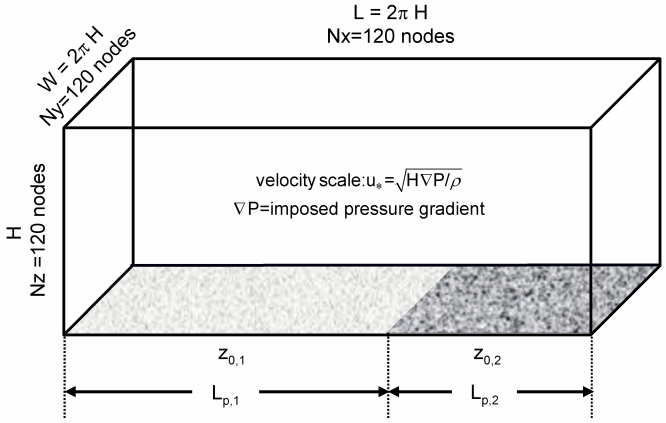

Figure 1. Simulation domain

A pseudo-spectral approach is used in the horizontal directions and a second order accurate centered-differences scheme in the vertical along with a staggered grid. Time advancement is performed with the fully explicit second order accurate Adams-Bashforth scheme. The dynamic computation of the coefficient at every time step is not necessary; the time-step for the Lagrangian dynamic model (Δt *i*n Eq.7) is chosen to be 5 times larger than the main LES timestep, greatly reducing the central processing unit (CPU) time requirements. Tests with a smaller time step Δt are performed to assure that this does not affect the model results. The bottom boundary condition is imposed using a modified version of the local law-of-the-wall to ensure that the average of the imposed wall stress is not erroneously high due to the local formulation. This is done using

$$\tau_w(x,y) = -\left[\frac{\kappa}{\ln(z/z_o)}\right]^2 \left(\left[\hat{\tilde{u}}(x,y,dz/2)\right]^2 + \left[\hat{\tilde{v}}(x,y,dz/2)\right]^2\right), \quad (8)$$

where u and v are the horizontal velocity components, κ is the von-Kraman constant, and z_o is the surface roughness.

A total of 28 simulations are performed; the simulations fall under 2 groups. All simulation parameters remain unchanged except the scale and roughness of the surface patches. The values of roughness length z_o are varied from 10^{-6}H to 10^{-3}H. In each case, only two roughness values $z_{o,1}$ and $z_{o,2}$ are used. The roughness ratio $z_{o,2}/z_{o,1}$ is set to 10 or 100. The patch length L_p varies between 0.21H and 3.14H; in addition, a homogeneous surface simulation with an effectively infinite patch length (due to the periodic boundary conditions in the horizontal directions) is performed.

The first group (A,B,C,D) consists of simulations with varying number of patches of equal size; therefore, the patch length varies between simulations but is fixed within a single simulation. For more information about the details and result from this group refer to Bou-Zeid *et al.* [4]. The second group (SR) consists of simulations where the patch length varies within a single simulation; i.e. surfaces with unequal-sized patches. Table 1 details the simulations parameters.

Table 1. Simulation cases and h_b and $z_{o,e}$ values determined from LES results

Simu-lation	# of patches	$L_{p,1}$/H	$L_{p,2}$/H	$z_{o,1}$/H, $z_{o,2}$/H	$\frac{z_{o,e\text{-LES}}}{H}10^3$	$\frac{h_{b\text{-LES}}}{H}$
A1	1	Infinite		10^{-6}	0.101	-
A2	2	3.14	3.14	$2.5\ 10^{-5}$, 2.510^{-4}	0.104	0.285
A4	4	1.57	1.57	$2.5\ 10^{-5}$, 2.510^{-4}	0.105	0.170
A6	6	1.045	1.045	$2.5\ 10^{-5}$, 2.510^{-4}	0.104	0.125
A8	8	0.785	0.785	$2.5\ 10^{-5}$, 2.510^{-4}	0.108	0.100
A12	12	0.523	0.523	$2.5\ 10^{-5}$, 2.510^{-4}	0.115	0.075
A20	20	0.314	0.314	$2.5\ 10^{-5}$, 2.510^{-4}	0.123	0.055
A30	30	0.209	0.209	$2.5\ 10^{-5}$, 2.510^{-4}	0.130	0.040
B2	2	3.14	3.14	10^{-4} , 10^{-3}	0.366	0.315
B4	4	1.57	1.57	10^{-4} , 10^{-3}	0.372	0.190
B8	8	0.785	0.785	10^{-4} , 10^{-3}	0.402	0.120
B20	20	0.314	0.314	10^{-4} , 10^{-3}	0.459	0.065
C2	2	3.14	3.14	10^{-5} , 10^{-3}	0.229	0.290
C4	4	1.57	1.57	10^{-5} , 10^{-3}	0.262	0.180
C8	8	0.785	0.785	10^{-5} , 10^{-3}	0.284	0.110
C20	20	0.314	0.314	10^{-5} , 10^{-3}	0.373	0.070
D2	2	3.14	3.14	10^{-6} , 10^{-4}	0.0255	0.250
D4	4	1.57	1.57	10^{-6} , 10^{-4}	0.0256	0.150
D8	8	0.785	0.785	10^{-6} , 10^{-4}	0.0300	0.088
D20	20	0.314	0.314	10^{-6} , 10^{-4}	0.0339	0.050
S07R93	2	0.44	5.84	10^{-5} , 10^{-4}	0.090	0.225
S12R88	2	0.75	5.525	10^{-5} , 10^{-4}	0.080	0.230
S25R75	2	1.57	4.71	10^{-5} , 10^{-4}	0.0632	0.240
S33R67	2	2.07	4.21	10^{-5} , 10^{-4}	0.058	0.240
S67R33	2	4.21	2.07	10^{-5} , 10^{-4}	0.028	0.260
S75R25	2	4.71	1.57	10^{-5} , 10^{-4}	0.023	0.265
S88R12	2	5.525	0.75	10^{-5} , 10^{-4}	0.017	0.305
S93R07	2	5.840	0.44	10^{-5} , 10^{-4}	0.0137	0.310

For the first group, finding a length scale L_p that characterizes the size of the patches is relatively straightforward since all patches in a single simulation are of equal size, this patch length is used as the characteristic heterogeneity or patch scale L_p. For the second group, the average of the streamwise lengths of the patches is used for L_p. This method is simple in the present case but might be

problematic to use in simulations where the streamwise direction varies.

Results from Simulation A1 were used to validate the code with the SGS model (previous versions of the code were validated with other SGS model, see Albertson and Parlange [15, 16] and Porté-Agel *et al.* [21]). One of the main functions of an SGS model being to dissipate the right amount of energy, it is crucial that an SGS model produces correct energy spectra for a given flow. In turbulent flow over rough walls, scaling arguments and experimental results suggest that the streamwise spectra should display a slope of -1 in the production range. In the inertial subrange, the Kolmogorov spectrum should be reproduced with its characteristic -5/3 slope. Fig. 2 depicts the streamwise spectra for simulation A1; the expected slopes are well reproduced by the Lagrangian dynamic scale-dependent SGS model.

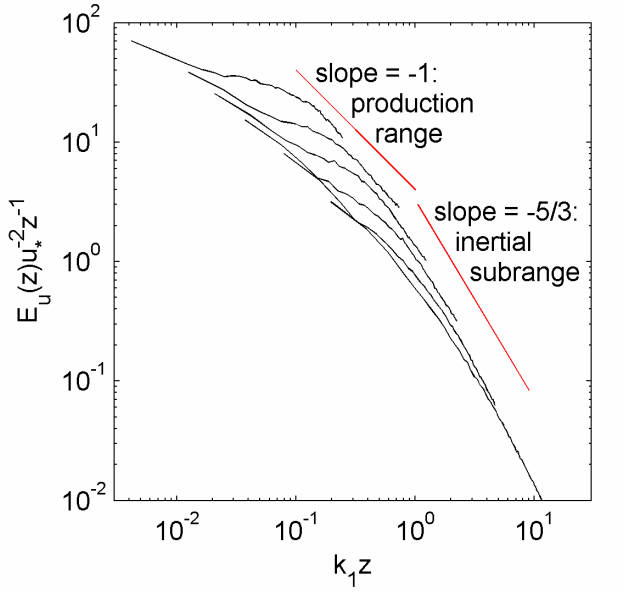

Figure 2. *u* velocity spectra versus k_1z; k_1 is the stream-wise wave number and *z* is the height. Each line represents the data for a selected height (at z/H of 0.0042, 0.0126, 0.021, 0.046, 0.130, or 0.267.

The numerical cost of the Lagrangian dynamic model exceeds the cost of the plane averaged scale-dependent dynamic model by about 6 percent only, mainly because the c_s is recomputed only every fifth time step. To justify the use of this more complicated but local c_s determination, the Smagorinsky coefficient has to be sensitive to the heterogeneity of the surface. To test this, the value of c_s averaged in the cross-stream direction is plotted versus x and z in Fig. 3 for simulation A2 (2 patches). The coefficient is divided by its average over horizontal planes to remove the effect of vertical variations and detect the sensitivity to horizontal variations. As is clear in Fig. 3, the value of the coefficient varies by up to 50 percent between the high-roughness and low-roughness patches near the ground and the effect of surface heterogeneity extends up to 0.05H into the domain. This illustrates the benefits of performing a local determination of the Smagorinsky coefficient in LES of complex flows.

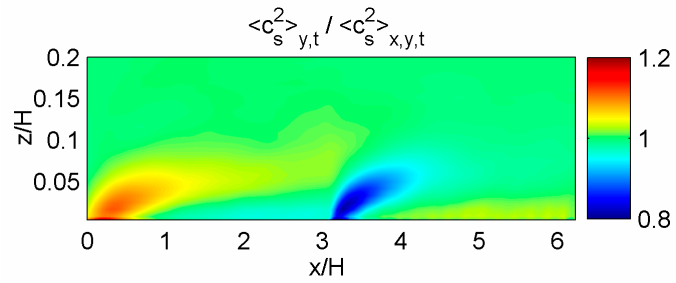

Figure 3. Sensitivity of the c_s coefficient to surface roughness (simulation A2)

The effective surface roughness ($z_{o,e}$) is determined by a least square fit between the measure streamwise velocity and the law of the wall expression (Fig. 4); the first six grid points from the wall are used in the fitting. For more details about the methods used to determine these parameters refer to Bou-Zeid *et al.* [4]. Results are presented in Table 1.

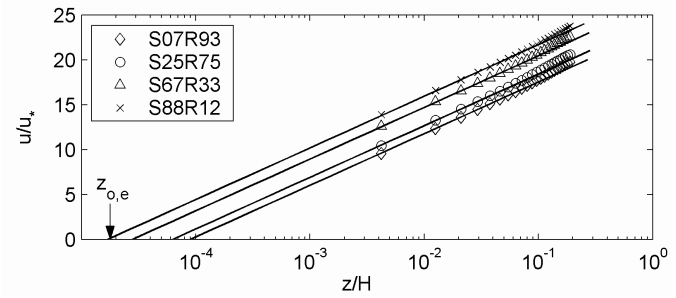

Figure 4. Equivalent surface roughness determined from velocity profiles, the straight line are the least square fits for the first six points

The blending height (h_b) is determined by computing the upper and lower quartiles of the mean profiles of the streamwise velocity at each height averaged over time and cross-stream direction y. Then, the vertical profiles of these quartiles are plotted and the blending height is defined as the height where the quartiles display a neck (Fig. 5). The determined values of h_b are shown in Table 1. The blending heights thus determined are plotted versus the length of the high roughness patch; results are shown in Fig. 6. The data was also plotted versus the low-roughness patch scale and the heterogeneity characteristic scale. The data was scattered in all plots.

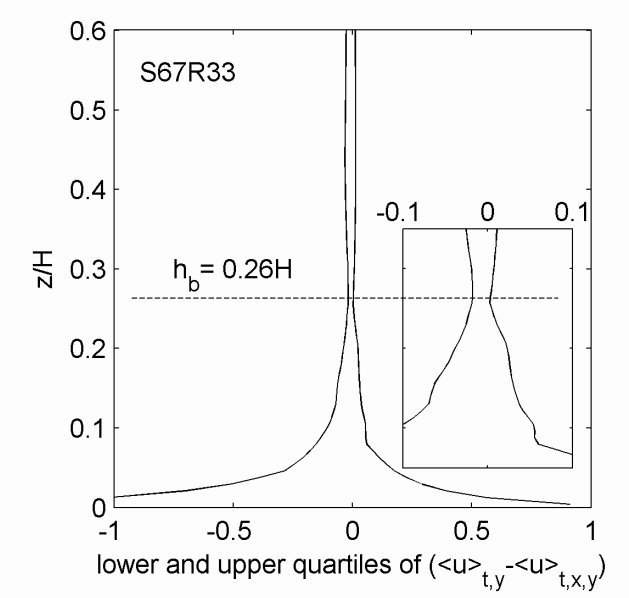

Figure 5. Determination of the blending height from the profiles of deviation velocity quartiles

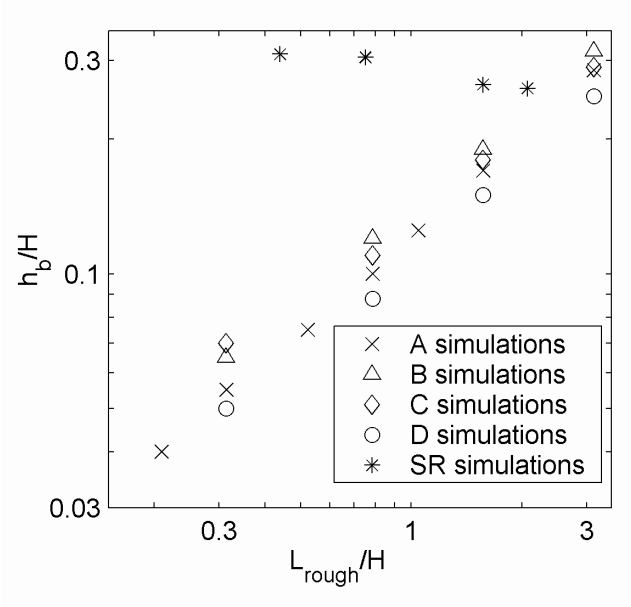

Figure 6. Blending height as a function of the high roughness patch length

INTERNAL BOUNDARY LAYER GROWTH

As the flow passes from one patch to another, an internal boundary layer (IBLs) emanates from the boundary of the patch. The flow inside the IBL is controlled by the underlying surface while the flow outside is controlled by the upstream patch and the flow in the outer region. The blending of surface heterogeneities by turbulent mixing in the flow is closely related to the formation and development of the internal boundary layers. As the IBL develops downstream and into the outer flow, its outermost parts are mixed by the turbulent eddies. The signature of the surface weakens as the distance from the wall increases and a point is reached where the IBL top is completely mixed with the outer flow and other IBLs; above that point the flow is statistically homogeneous in the wall-parallel direction.

To better understand the physical mechanisms controlling the growth of the IBL, a classic scaling argument was revisited [4]. Briefly reviewing, this approach estimates the growth of the boundary layer using a diffusion analogy. Scaling arguments yield:

$$\frac{\partial \delta_{\mathrm{IBL}}}{\partial x} \sim \frac{\text{upward diffusion velocity}}{\text{streamwise convection velocity}} \sim \frac{w_{\mathrm{rms}}}{\left\langle u(\delta_{\mathrm{IBL}})\right\rangle} \tag{9}$$

where x is the downstream distance, $\langle u(\delta_{\mathrm{IBL}})\rangle$ the mean stream-wise velocity at the top of the IBL, and w_{rms} the standard deviation (the root mean square) of the vertical velocity. w_{rms} can be approximated by u_* (from LES data, for the lower 20% of the ABL, $w_{\mathrm{rms}} \sim 0.95u_*$) whereas the mean stream-wise velocity can be estimated from an effective log profile. Developing this scaling equation and integrating from ($\delta_{\mathrm{IBL}} = z_{\mathrm{o,e}}$ at x = 0) to (δ_{IBL} at x) yields the following relation between the IBL depth and the effective surface roughness $z_{\mathrm{o,e}}$

$$\delta_{\mathrm{IBL}}\left[\ln\left(\frac{\delta_{\mathrm{IBL}}}{z_{\mathrm{o,e}}}\right)-1\right] = C\,\kappa x \tag{10}$$

C is an empirical constant, κ the von-Karman constant. δ_{IBL} determined from this equation can be compared to δ_{IBL} determined from LES (using the $d\langle u\rangle_{\mathrm{t,y}}/dz = d\langle u\rangle_{\mathrm{t,x,y}}/dz$ method) to determined the empirical coefficient C. As shown in Bou-Zeid *et al.* [4], a value of 0.85 for C can successfully predict δ_{IBL}.

BLENDING HEIGHT

Extension of the IBL growth equation to predict blending height can be successful if the downstream distance at which the IBL top reaches the blending height can be determined. To explore this, contour plots of the non-dimensional u gradient $\kappa z/u_*$ ($d\langle u\rangle_{\mathrm{y,t}}/dz$) were inspected along with δ_{IBL} determined from Eq. (10). In all simulations, when the IBL is allowed to grow until a downstream distance roughly equal to twice the patch length, the blending height is reached (Bou-Zeid *et al.*, 2004). Hence, the blending height can be defined through

$$h_{\mathrm{b}} = \delta_{\mathrm{IBL}}(x = \alpha L_{\mathrm{p}}) \text{ with } \alpha \approx 2\,. \tag{11}$$

Note that the determination of α is empirical and further tests are needed to verify if the value of this coefficient is relatively constant for different types of patch distributions. Combining with Eq. (10) and C=0.85 yields the following relationship between the blending height h_b, characteristic patch length L_p, and effective surface roughness $z_{\mathrm{o,e}}$:

$$h_{\mathrm{b}}\left[\ln\left(\frac{h_{\mathrm{b}}}{z_{o,e}}\right)-1\right] = 0.85\kappa(2L_{\mathrm{p}})\,. \tag{12}$$

Fig. 7 compares the h_b predicted by this equation to the values determined from LES data; it depicts blending height

versus patch length (divided by the equivalent surface roughness to reduce the number of variables to 2, $h_b/z_{o,e}$ and $L_p/z_{o,e}$). The symbols are the heights determined from LES data; the solid line is the prediction of Eq. (12). The comparison is quite good indicating that Eq. (12) can be used to predict the blending height for all patch cases considered in this study.

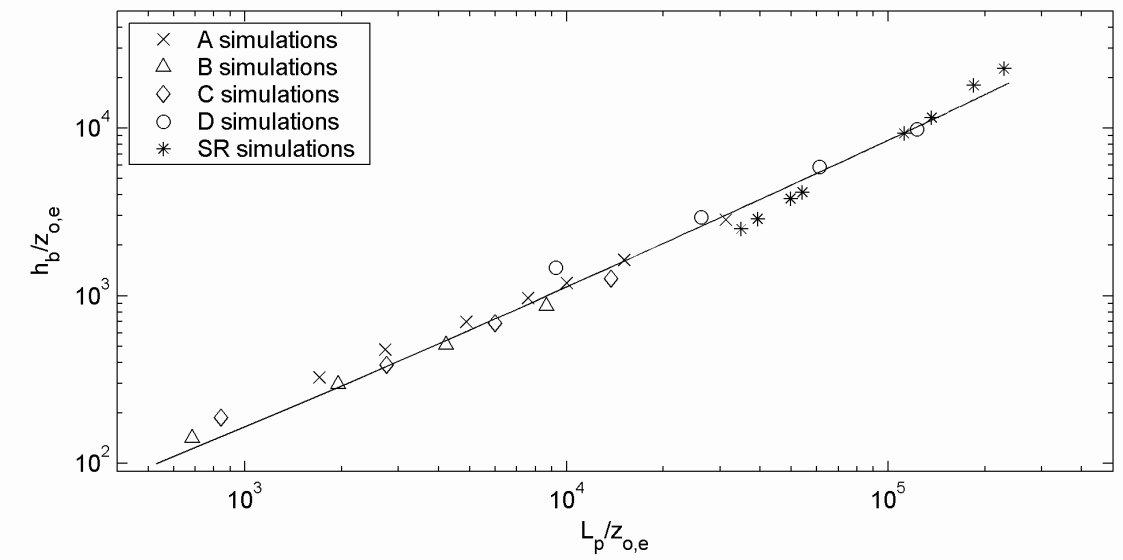

Figure 7. Normalized mixing height versus patch length for all simulations fitted with a curve of the form $h_b[\ln(h_b/z_o)-1]=1.7\,\kappa L_p$.

EFFECTIVE SURFACE ROUGHNESS

Eq. (12) used to compute the blending height involves the value of the equivalent surface roughness $z_{o,e}$. The values for the surface roughness used till now were obtained from LES data; however, a parameterization for $z_{o,e}$ is required to allow computation of the blending height without any need for flow measurements; moreover, a parameterization of $z_{o,e}$ is important by itself for the reasons discussed in the introduction.

The proposed approach is based on work by Wieringa [25], Mason [26], and Claussen [3]. A slight modification, that becomes important for small patch scales, was proposed and tested versus LES results by Bou-Zeid *et al.* [4]; that study focused on the first group of simulations A-D. In this paper, tests are performed with simulations where the patch scales can vary in a single simulation; thus getting closer to realistic situations. Future work will consider patches with random sizes and roughness heights.

The net friction force over a heterogeneous area is written as the sum of friction forces over each patch in the area

$$A_{\text{total}}\tau_{\text{total}} = \sum_{i=1}^{N} A_i \tau_i \ , \tag{13}$$

where N is the number of patches, A_{total} is the total area considered, and A_i is the surface of patch i. If the patches are assumed to be big enough so that the flow is in equilibrium with the underlying surface over most of the patch, the average surface stress over a patch can be expressed using the law-of-the-wall using

$$\left(\frac{u_e \kappa}{\ln\left(\frac{z}{z_{o,e}}\right)}\right)^2 = \sum_{i=1}^{N} f_i \left(\frac{u_i \kappa}{\ln\left(\frac{z}{z_{o,i}}\right)}\right)^2 , \tag{14}$$

where u_e is the velocity averaged over the whole domain and $z_{o,e}$ is the equivalent surface roughness that is to be determined by this procedure. Moreover, u_i and $z_{o,i}$ are the equilibrium velocity and the surface roughness of patch i and f_i is the fraction of the total area covered by patch i ($f_i = A_i/A_{\text{total}}$). Following references [25] and [26], the above equation is evaluated at the blending height h_b where one may assume that the flow velocity is homogeneous over all the area ($u_i \approx u_e$ for any patch). The equation reduces to

$$\frac{1}{\left(\ln\frac{h_b}{z_{o,e}}\right)^2} = \sum_{i=1}^{N} f_i \frac{1}{\left(\ln\frac{h_b}{z_{o,i}}\right)^2} . \tag{15}$$

Eqs. (12) and (15) can be combined to yield an equation for h_b that has to be solved iteratively:

$$\left(\frac{h_b}{1.7\kappa L_p + h_b}\right)^2 = \sum_{i=1}^{N} f_i \frac{1}{\left(\ln\frac{h_b}{z_{o,i}}\right)^2} . \tag{16}$$

The value of $z_{o,e}$ can then be computed from Eq. (12) according to:

$$z_{o,e} = h_b \exp\left[-\frac{1.7\kappa L_p}{h_b} - 1\right]. \quad (17)$$

Next, this model (i.e. Eqs, (16) and (17)) is used to estimate the equivalent surface roughness for the LES runs, and the results are compared to the effective surface roughness determined from LES data. Fig. 8 presents the ratio z_o^{model}/z_o^{LES} when plotted versus z_o^{LES}. A value of 1 (thick black line) indicates a perfect model. All model estimates are within 25 percent of the LES results suggesting that the proposed parameterization is quite successful in predicting the equivalent surface roughness for simple patch distributions. In future work, tests will be performed to see if the performance of the parameterization is as satisfactory with highly random distributions of roughness. The more realistic configurations that will be tested include patches of different sizes and complex configurations. An important challenge in such situation is to be able to find a single characteristic scale for surface heterogeneity. See reference [27] for an interesting discussion of approaches that can be used to obtain such a characteristic patch length.

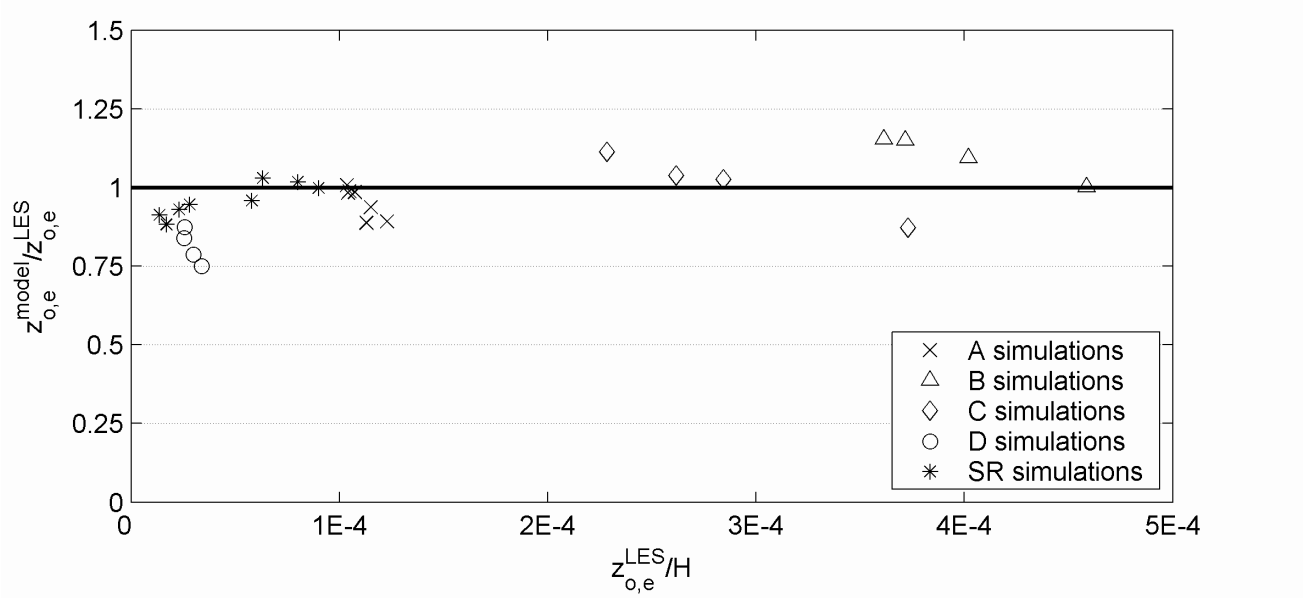

Figure 8. Comparison of equivalent surface roughness estimated by the analytical model (Eqs. (15) and (16)) to LES values (Table 1). The thick line corresponds to $z_o^{model}=z_o^{LES}$ (perfect fit).

CONCLUSIONS

LES was used to simulate turbulent wall-bounded flows with heterogeneous roughness distributions. Two groups of simulation were performed with varying roughness heights and heterogeneity scales. Plots of the dynamically-determined Smagorinsky coefficient used in the SGS model indicate that it is quite sensitive to the surface roughness thus validating the need for a model where c_s is determined locally such as the Lagrangian model implemented here. A parameterization for internal boundary layer growth rate was developed and used to predict the blending height, and combined with an equation for surface stresses. This resulted in a system of 2 equations for the blending height and the effective surface roughness. The predictions of this parameterization were successfully compared to LES values suggesting that the parameterization can be used to predict effective surface roughness from basic patch characteristics, namely patch scale and roughness heights. The effective surface roughness heights from the parameterization were within 25 percent of LES values.

ACKNOWLEDGMENTS

This study was funded by NSF under EAR-9909679 and by agreement number R828771-0-01 from the U.S. Environmental Protection Agency's Science to Achieve Results (STAR) program. The authors are thankful for the Scientific Computing Division of the National Center for Atmospheric Research (NCAR) for the use of their computer clusters.

REFERENCES

[1] Meneveau, C., Lund, T., and Cabot, W., 1996, "A Lagrangian dynamic subgrid-scale model of turbulence." J. of Fluid Mechanics, **319**, pp. 353-385.

[2] Miyake, M., 1965, “Transformation of the atmospheric boundary layer over inhomogeneous surfaces.” University of Washington, Department of Atmospheric Sciences, Report AD 626630.

[3] Claussen, M, “Estimation of areally-averaged surface fluxes”, Boundary Layer Meteoroogy, **54**, pp. 387-410.

[4] Bou-Zeid, E., Meneveau, M, and Parlange, MB, 2004, “Large eddy simulation of neutral atmospheric boundary layer flow over heterogeneous surfaces: blending height and effective surface roughness,” Water Resources Research, **40,** W02505, doi:10.1029/2003Wr002475.

[5] Antonia, R.A., and Luxton, R.E., 1971, “The response of a turbulent boundary layer to a step change in surface roughness. part 1. smooth to rough,” J. of Fluid Mechanics, **48**, pp. 721-761.

[6] Antonia, R.A., and Luxton, R.E., 1972, “The response of a turbulent boundary layer to a step change in surface roughness. part 2. rough to smooth,” J. of Fluid Mechanics, **53**, pp. 735-757.

[7] Fredsoe, J., Sumer, B.M., Laursen, T.S., and Pedersen, C., 1993, “Experimental investigation of wave boundary layers with a sudden change in roughness,” J. of Fluid Mechanics, **252**, pp. 117–146.

[8] Belcher, S.E., Jerram, N., and Hunt, J.C.R., 2003, “Adjustment of a turbulent boundary layer to a canopy of roughness elements,” J. of Fluid Mechanics, **488**, pp. 369–398.

[9] Glendening, J.W., and Lin, C.L. “Large Eddy Simulation of internal boundary layers created by a change in surface roughness,”, J. of Atmospheric Sciences, **59**, pp. 1697-1711.

[10] Hechtel, L.M., Stull, R.B., and Moeng, C.-H., 1990, “The effects of nonhomogeneous surface fluxes on the convective boundary-layer: a case study using large-eddy simulation,” J. of Atmospheric Sciences, **47**, pp. 1721-1741.

[11] Shen, S.H., and Leclerc, M.Y., 1995, “How large must surface inhomogeneities be before they influence the convective boundary layer structures? A case study,” Quarterly Journal of the Royal Meteorological Society, **121**, pp. 1209-1228.

[12] Khanna, S., and Brasseur, J.B., 1997, “Analysis of Monin-Obukhov similarity from large-eddy simulation,” J. Fluid Mechanics, **345**, pp. 251-286.

[13] Avissar, R., Eloranta, E.W., Gurer, K., and Tripoli, G.J., 1998, “An evaluation of the large-eddy simulation option of the regional modeling system in simulating a convective boundary layer: a FIFE case study,” J. of Atmospheric Sciences, **55**, pp. 1109-1130.

[14] Albertson, J.D., and Parlange, M.B., 1999a, “Natural integration of scalar fluxes from complex terrain,” Advances in Water Resources, **23**, pp. 239-252.

[15] Albertson, J.D., and Parlange, M.B., 1999b, “Surface length-scales and shear stress: implications for land-atmosphere interaction over complex terrain,” Water Resources Research, **35 (7)**, pp. 2121-2132.

[16] Lesieur, M., and Métais O., 1996, “New trends in large-eddy simulations of turbulence,” Annual Review of Fluid Mechanics, **28**, pp. 45-82.

[17] Pope S.B., 2000, *Turbulent Flows*, Cambridge University Press, Cambridge, UK.

[18] Lilly, D.K. 1967, “The representation of small scale turbulence in numerical simulation experiments,” *Proc., IBM Scientific Computing Symposium on Environmental Sciences*, p. 195.

[19] Germano, M., Piomelli, U., Moin, P., and Cabot, W., 1991, “A dynamic subgrid-scale eddy viscosity model,”, Physics of Fluids A, **3**, pp. 1760-1765.

[20] Meneveau, C., and Katz, J., 2000, “Scale-invariance and turbulence models for large-eddy simulation,” Annual Review of Fluid Mechanics, **32**, pp. 1-32.

[21] Porté-Agel, F., Meneveau, C., and Parlange, M.B, 2000, “A scale-dependent dynamic model for large-eddy simulation: application to a neutral atmospheric boundary layer,” J. of Fluid Mechanics, **415**, pp. 261-284.

[22] Bradley, E.F., 1968, “A micrometeorological study of velocity profiles and surface drag in the region modified by a change in surface roughness,” Quarterly Journal of the Royal Meteorological Society, **94**, pp. 361-379.

[23] Rao, K.S., Wyngaard, J.C., and Coté, O.R., 1973, “The structure of the two-dimensional internal boundary layer over a sudden change of surface roughness,” Journal of Atmospheric Sciences, **31**, pp. 738-746.

[24] Garratt, J.R., 1990, “The internal boundary layer – a review,” Boundary Layer Meteorology, **50**, pp. 171-203.

[25] Wieringa, J., 1986, “Roughness-dependent geographical interpolation of surface wind speed averages,” Quarterly Journal of the Royal Meteorological Society, **112**, pp. 867-889.

[26] Mason, P.J., 1988, “The formation of areally-averaged roughness lengths,” Quarterly Journal of the Royal Meteorological Society, **114**, pp. 399-420.

[27] Brutsaert, W., 1998, “Land-surface water vapor and sensible heat flux: spatial variability, homogeneity, and measurement scales,” Water Resources Research, **34(10)**, pp. 2433-2442.